

Exploring the Impact of Mountain Urban Characteristics on Housing Prices: A Study Utilizing Street View Visual Features

Xuhui Cui¹, Sha Li¹, Zhen Li², Zhaohan Dong³

¹ China University of Mining and Technology, Xuzhou 221000, China - (ts22190075a31tm, 5979)@cumt.edu.cn

² Defense Engineering Institute, AMS, PLA, Beijing 100850, China - lzgirls2024@163.com

³ Central and Southern China Municipal Engineering Design & Research Institute Co., Ltd., Hangzhou 310000, China - 19816240130@163.com

Keywords: Mountain City, Housing Prices, Visual Perception, Street View, Deep Learning, Grad-CAM.

Abstract

Urban mountains shape the spatial and landscape structure of cities. Rapid urbanization and an increase in real estate developments have led to the erosion of unique urban landscape features. However, mountain cities boast distinctive terrain and landscapes, endowing them with a wealth of scenic resources and aesthetic appeal. Residents' growing concern for their living environment's quality and scenic beauty impacts property values during urban development. Mountain landscapes, vital natural elements of mountain cities, are studied less in their effect on housing prices compared to water features and urban greenery, despite their unique appeal to residents. This study integrates various sources of urban data with subjective analysis of human behavior and the multiscale geographically weighted regression (MGWR) to assess the factors affecting housing prices in mountain cities. It examines the spatial distribution and influence of street view elements on property values and uses gradient-weighted class activation mapping (Grad-CAM) to analyze visual perception characteristics of street views. Research findings reveal urban street view elements, especially mountain views, significantly affect housing prices with pronounced spatial heterogeneity, this spatial unevenness also shifts with urban development, influencing housing prices.

1. Introduction

As a country dominated by mountainous landscapes, the majority of China's cities are built on or surrounded by mountains. This inherent geographical trait not only endows these cities with abundant scenic vistas but also deep aesthetic significance.

Over recent decades, the rapid pace of urbanization and expansion has precipitated an increase in the scale of construction projects and building heights. Concurrently, the character of urban landscapes in many Chinese cities has been fading, leading to a notable trend of homogenization, where the singular landscape characteristics have become increasingly prevalent. Mountains, integral to the ecological framework and natural architecture of urban planning, significantly shape the spatial structure, layout, and visual character of urban environments (Qi et al., 2022). Globally, mountain landscapes are revered, with peaks representing idealized values and aesthetic principles in Western thought (Beza, 2010), and associated with sacred symbolism and beliefs (Yu et al., 2023). In accordance with "Feng Shui" principles, there is a cultural tendency to favor homes with a southern exposure and mountains to the rear, promoting harmony between humans and nature (Mak and Thomas Ng, 2005). This practice has influenced the choice of locations for many habitable areas (Liu et al., 2023). However, the accelerated pace of urban development and the real estate surge have threatened the uniqueness of cities known for their picturesque and habitable mountainous environments, leading to a risk of landscape characteristics uniformity (Yu et al., 2023).

As cities expand, the involvement of real estate developers in urban economic growth and territorial expansion becomes evident. This development coincides with residents' growing concern for the quality and aesthetic appeal of their surrounding living environments, often influencing their decisions in

housing purchases and consumption behaviors (Jim and Chen, 2009). Factors such as attractive landscapes, expansive views, and sufficient greenery are known to enhance property values (Yamagata et al., 2016). Additionally, the visual appearance and perceived image of neighborhood streets play a pivotal role in shaping residents' impressions of their communities (Xu et al., 2022). The quality of street view can directly or indirectly impact community property values, while broader features like urban mountains or harbor views serve as significant attractors of property values (Jim and Chen, 2009). Although in some Chinese cities, mountain landscapes have significantly boosted overall housing prices (Wen et al., 2015), the influence of mountain landscapes on housing prices shows marked spatial heterogeneity, more so than the impacts of urban river views (Liu et al., 2019). Consequently, the effect of mountain landscapes on urban housing prices, compared to other urban landscape elements such as natural water bodies and street greenery, has not been fully investigated.

Housing, as a product marked by its heterogeneity, is influenced by a myriad of factors, including landscapes, as well as by its structural characteristics and geographical location, all of which significantly affect price levels (Jim and Chen, 2006). The presence of essential local infrastructure, such as schools, hospitals, and transportation networks, also plays a pivotal role in shaping residents' willingness to pay for properties (Chin and Foong, 2006; Kopczevska and Lewandowska, 2018). While foundational data have traditionally underpinned studies on the determinants of housing prices, recent research efforts have started to draw connections between urban property prices and the unique features of certain cities, like the "Shan Shui" landscapes in Chongqing, China (Liu et al., 2019). Nonetheless, studies that utilize street view imagery and human perception data to delve into how distinct urban features, including landscapes, influence housing prices are still relatively infrequent.

The aim of this study is to utilize urban data and human perceptions to discern factors impacting housing prices in mountain cities. Objectives include: (1) developing a regression model with street view elements for Tai'an to uncover price determinants; (2) analyzing the influence of mountain city environments on housing prices and their spatial patterns; (3) applying gradient-weighted class activation visualization to identify commonalities in human-machine observations.

This study area, with sufficient conditions for mountain viewing, well-developed public service infrastructure, and rich open data showcasing the city's current state, was chosen to investigate the influence of diverse human behaviors and urban data on housing prices in mountain urban areas, as presented in Figure 2.

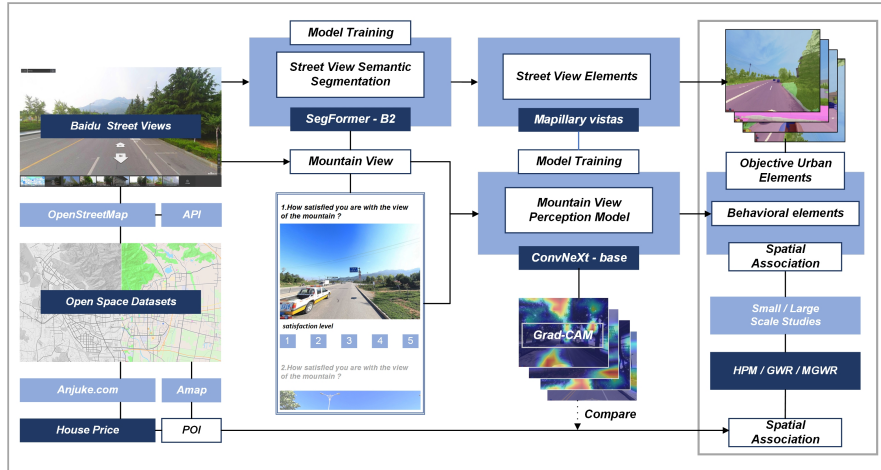


Figure 1. Research framework and workflow.

2. Data and Methodology

This study delineated a methodological framework to assess housing price determinants in mountain city, as shown in Figure 1. We amalgamated data from varied sources, including road networks, Baidu Street View imagery, housing price metrics, and points of interest. Street view element variables were extracted from street view imagery using semantic segmentation, while a subset of mountain view images underwent analysis through an impression evaluation model, grounded in human perception data. Employing spatial regression model, the study investigates spatial correlations between behavioral and objective datasets across the study area. Grad-CAM further elucidates the interplay between human perception and housing price data, revealing perceptual commonalities.

2.1 Study Area

In this study, we focused on the central urban district of Tai'an City, spanning approximately 207.7 km², adjacent to the Mount Tai Scenic Spot. Mount Tai, standing at 1,545 meters and renowned as one of China's most significant mountains, has been honored as "the most revered" of the Five Great Mountains. It was listed as a World Natural Heritage site in 1987 (Zhang and Zhang, 2019), underscoring its cultural and environmental significance.

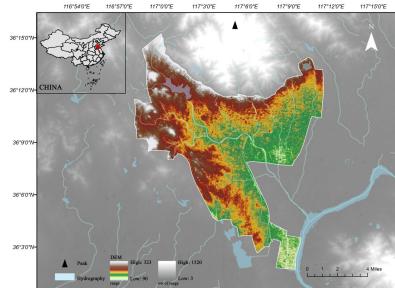


Figure 2. Study area.

2.2 Data Source

2.2.1 Housing Prices: Utilizing a web crawler on (Anjuke.com), data on pre-owned housing sales in the central district of Tai'an City for 2023 were collected, including attributes such as community address, construction year, floor area ratio, greening rate, and number of households. Data cleansing eliminated duplicates and null values, yielding records for 1,177 community housing prices. Subsequent analysis, visualized in Figure 3, elucidated the spatial distribution and aggregation patterns of housing prices. In the central district of Tai'an, housing prices exhibited a semicircular distribution congruent with the mountainous terrain, peaking in areas proximal to the northern mountains. Conversely, the southern city regions showed a decline in community density and associated housing prices.

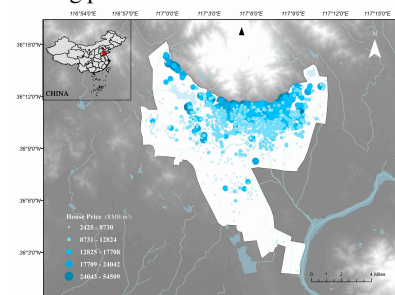


Figure 3. Study area housing price map.

2.2.2 Open Space: The road network data for the city of Tai'an was extracted from the OpenStreetMap (OSM) platform to support the collection of street view imagery and to establish spatial associations between community locations and points of interest (POIs). Subsequently, POIs in the central district of Tai'an were collected using the Amap Open Platform, enabling the delineation of facility attributes near residential areas. This effort spanned various functional categories, with a focus on education, healthcare, and government services. The process culminated in the aggregation of 8,781 POIs, each accurately documented with location details.

2.2.3 Street View Images: Imagery for this study was obtained from Baidu Street View (BSV). Street view sampling points were generated every 50 meters using ArcMap 10.7, and images were retrieved via Baidu Maps' Application Programming Interface (API). Due to the varying orientations of collection vehicles, images at each point were captured facing four cardinal directions (0°, 90°, 180°, 270°) at a resolution of 1024 x 700 pixels, totaling 43,680 images.

2.3 Method

2.3.1 Street View Elements Extraction: The study used the SegFormer-B2 model for semantic segmentation of street scenes, known for its validated effectiveness on relevant datasets (Xie et al., 2021), with the module depicted in Figure 4. The training was performed using the Pascal VOC pre-trained weights and the AdamW optimizer, known for its effectiveness on large datasets, with a momentum of 0.9 and an initial learning rate of 0.0001, ensuring improved performance and stability (Everingham et al., 2015; Ilya Loshchilov, 2019). The training process included 300 epochs with an image input size of 512x512 pixels. Significantly, the Mapillary Vistas Dataset, embodying a rich array of landscapes including mountainous terrains and urban scenes, was selected for model training, resonating with the study's emphasis on mountain urban environments (Neuhold et al., 2017).

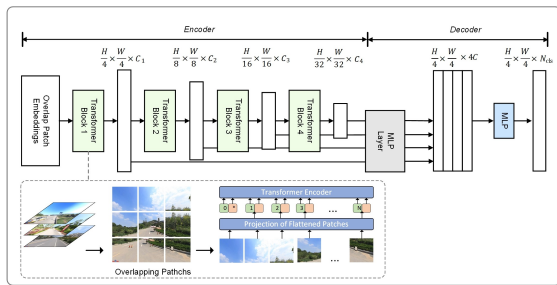


Figure 4. SegFormer-B2 module diagram.

This research employed classification indices from the street view dataset (Neuhold et al., 2017) to scrutinize the impact of various elements, natural (mountains, sky, vegetation, water), constructed (buildings), and flat surfaces on housing prices. Quantification of these distinct components enabled the derivation of objective metrics to ascertain their influence on property valuations.

2.3.2 Human Perception Score Extraction: A survey was conducted using the Tencent questionnaire platform (<https://wj.qq.com/>) to evaluate volunteer satisfaction with images of mountain views selected from segmented street view imagery. From this selection, 500 images containing mountain elements were randomly chosen for evaluation. Each participant rated their satisfaction on a five-point scale across 20 questionnaire sets (Joshi et al., 2015), each featuring 25 unique mountain images. Post-survey, data cleansing led to the calculation of average satisfaction scores per image and across all images. Satisfaction levels for each image were then categorized based on the standard deviation of these average scores, facilitating an analytical framework for interpreting perceptions of mountain views in urban landscapes.

We evaluated the street view images based on human perceptual scores using the ConvNeXt-base model, which was trained on satisfaction survey images with satisfaction levels as the target criteria. Known for its high accuracy and fast inference

capabilities, the structure of this model was shown in Figure 5 (Liu et al., 2022).

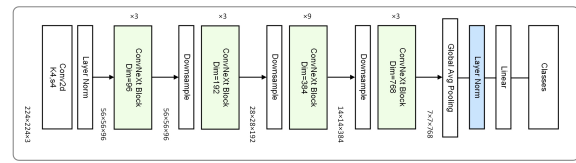


Figure 5. ConvNeXt-base module diagram.

2.3.3 Spatial Association: In this study, we established spatial associations among street view elements, community structural characteristics, and their proximate attributes. Data on factors like building age, floor area ratio, greenery rate, and household count were extracted as structural characteristics. A 500-meter buffer was used to gauge the community's surrounding characteristics, calculating averages to determine objective neighborhood characteristics (Sung et al., 2014). The neighborhood profile included variables such as the density of parks and government facilities within a 1-kilometer radius. Mountain view observations connected the nearest community data through image sampling points. The Manhattan distance metric provided a realistic assessment of pedestrian travel in urban blocks, linking community attributes more accurately to their spatial context.

2.3.4 Hedonic Price Model: Housing prices were analyzed using the Hedonic Pricing Model (HPM), which segments price determinants into attributes with differential impact levels. Research has extensively adopted this method for assessing the built environment's effect on property values (Chen et al., 2020; Xu et al., 2022). Influences on housing prices were acknowledged to extend beyond structural characteristics, such as building age and floor area ratio, to include proximate features like community location and surrounding scenery (Liao et al., 2022). Primarily based on Ordinary Least Squares (OLS) regression, the HPM implied a linear relationship between the price and a set of various predictive variables. The HPM employed in this study was expressed in Eq1:

$$P_i = \beta_0 + \sum_{j=1}^k \beta_j x_{ij} + \epsilon_i \quad (1)$$

Where P_i = the price of the i th property
 β_0 = the intercept
 k = the total number of explanatory variables
 x_{ij} = the j th characteristic of the i th property
 β_j = the regression coefficient for each characteristic
 ϵ_i = the error term

2.3.5 Spatial Regression Analysis: Spatial variability, typically unaccounted for in HPM applying OLS, conceals the nuances of spatial relationships. This study rectified this by integrating the geographically weighted regression (GWR) and the multiscale geographically weighted regression (MGWR), with GWR elucidating spatial heterogeneity through localized parameters. The GWR model's implementation was as specified in Eq2:

$$P_i = \beta_0 + \sum_{j=1}^k \beta_j(u_i, v_i) x_{ij} + \epsilon_i \quad (2)$$

Where P_i = the price of the i th property
 β_0 = the location-specific intercept term
 $\beta_j(u_i, v_i)$ = the spatially varying coefficient for the j th explanatory variable
 x_{ij} = the j th characteristic of the i th property
 ϵ_i = the error term at the i th location

In the MGWR model, flexibility was introduced by permitting variable-specific bandwidths, unlike GWR which assumes a uniform bandwidth across all variables. The equation governing the MGWR model was delineated as follows:

$$P_i = \beta_0(u_i, v_i) + \sum_{j=1}^k \beta_{ji}(u_i, v_i)x_{ij} + \epsilon_i \quad (3)$$

Where P_i = the price of the i th property
 $\beta_0(u_i, v_i)$ = the spatially varying intercept term
 $\beta_{ji}(u_i, v_i)$ = the spatially varying coefficient for the j th explanatory variable
 x_{ij} = the j th characteristic of the i th property
 ϵ_i = the error term at the i th location

2.3.6 Visualization of Class Activation Map: We used a ConvNeXt-base model trained with SVIs satisfaction survey data to classify the satisfaction levels of images. This approach allowed for the exploration of dynamics in human perception through Class Activation Map (CAM) visualization of images from various satisfaction categories. The study utilized CAM for deep visualization, identifying focal points in images to clarify the model's focus on SVIs. Grad-CAM, with model weights, generated heat maps for class activation, improving model interpretability (Zhao et al., 2024). This method highlighted the visual allure of street view elements and revealed the model's perceptual priorities in mountain urban settings.

3. Results

3.1 Spatial Distribution of Urban Street View Elements

The SegFormer-B2 semantic segmentation model achieved an accuracy of 89.40%. Using the natural breaks method, we mapped the spatial distributions of six key elements: building view index (BVI), flat view index (FVI), mountain view index (MVI), sky view index (SVI), water view index (WVI) and green view index (GVI), with their average values calculated to be 0.09871, 0.21299, 0.00086, 0.32914, 0.00031 and 0.23410. Figure 6 showed that higher BVI values were predominant in the core areas of the central urban district, characterized by dense construction and the highest concentration of residential communities. Conversely, SVI displayed an inverse distribution pattern, gradually increasing from the core area to the periphery. GVI's distribution was dense not only in the central area but also significantly high along the northern mountainous roads, as well as in the western and southern suburbs. MVI was primarily concentrated along the northern mountain line, with other areas presenting lower and average levels.

3.2 Correlation Analysis of Human Perception Scores

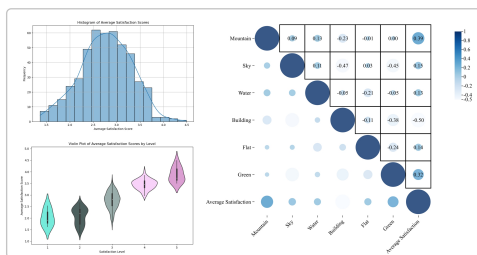


Figure 7. Pearson correlation analysis of perception scores.

From 534 valid questionnaire responses, including 238 males and 296 females, an average satisfaction score of 2.77 emerged, aligning with a normal distribution trend and a standard

deviation of 0.54. This facilitated dividing satisfaction into five levels, with volunteers showing lower preferences for extreme mountain view ratings. Pearson correlation analysis linked street view elements to mountain view satisfaction, as illustrated in Figure 7, revealing positive correlations with mountains (0.39) and greenery (0.32), and a strong negative correlation with buildings (-0.50).

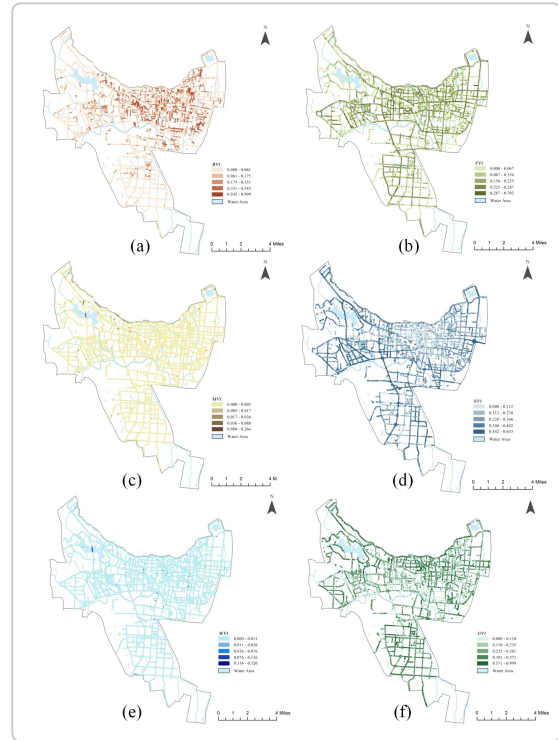


Figure 6. The spatial distribution of urban street view elements. (a) building view index; (b) flat view index; (c) mountain view index; (d) sky view index; (e) water view index; (f) green view index.

Acknowledging a general preference for moderation, a three-classification model was formulated to assess satisfaction with mountain views, dividing photo data into an 80-20 split for training and testing. The model achieved a 66.70% accuracy after 300 epochs, with a learning rate decreasing from 0.0002 to 0.0001. Using the Adam optimizer enabled satisfactory performance even on small datasets (Diederik P. Kingma, 2017). Satisfaction for street attractions was predicted across 43,680 SVIs. For clearer results presentation, we applied the natural breaks method in ArcMap 10.7 to relate satisfaction scores with housing prices, as shown in Figure 8. High visual satisfaction areas from mountain views, primarily at elevated locations except for the central city and north along the mountain ring, aligned more closely with housing prices.

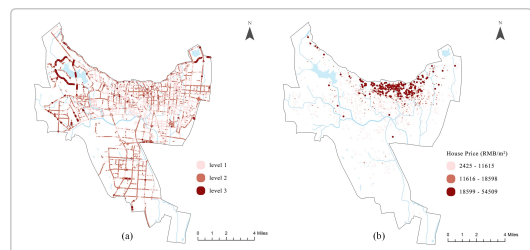


Figure 8. Comparison of predicted satisfaction and housing prices, including housing prices (RMB/m²) for the location shown on the right. Levels of satisfaction perception: Level 1 (Low), Level 2 (Medium), Level 3 (High).

3.3 Results of Spatial Regression Analyses

Before developing the spatial regression model, we evaluated the variance inflation factors (VIF) of identified variables to detect multicollinearity, ensuring robustness. Variables demonstrating no multicollinearity, indicated by a VIF less than 5, were selected for inclusion in the model (Marquardt, 1970). Finally, we obtained descriptive information on variables that included structural characteristics, neighborhood characteristics, and street element characteristics, as detailed in Appendix Table A1.

Model	Macro scale		Mountain view	
	R^2	R^2_{adj}	R^2	R^2_{adj}
HPM	0.346	0.334	0.419	0.392
GWR	0.582	0.521	0.893	0.841
MGWR	0.613	0.560	0.911	0.881

Table 1. Comparison of models.

Table 1 demonstrated that both the R^2 and adjusted R^2 of the GWR and MGWR models outperformed those of the HPM. In the broader study, GWR and MGWR models explained 58.2% and 61.3% of the variance in housing prices, respectively. In the mountain view area, GWR and MGWR models explained 89.3% and 91.1% of the variance, respectively. Overall, MGWR model surpassed traditional HPM and GWR model, making it the preferred regression model for this study.

Variables	Model 1	Model 2
	(macro scale)	(mountain view)
	MGWR	MGWR
Structural characteristics		
AGE	152	43
FR	911	54
HS	373	43
GR	1171	296
Neighborhood characteristics		
D_Bus	436	88
D_Hospital	112	144
D_School	1152	48
D_Government	1176	86
D_Park	1176	51
N_Government	361	119
N_Park	1176	474
Street element characteristics		
MVI	193	177
BVI	80	43
FVI	975	463
SVI	293	425
WVI	951	271
GVI	268	459

Table 2. Comparison of parameter bandwidth (macro scale bandwidth = 1177, mountain view area bandwidth = 475).

Variables	Model 1 (macro scale)		Model 2 (mountain view)	
	$E_{st.}$	SE	$E_{st.}$	SE
Structural characteristics				
AGE	0.023	0.035	0.138**	0.040
FR	0.029	0.024	0.171***	0.040
HS	-0.111***	0.027	-0.314***	0.041
GR	0.124***	0.035	0.277***	0.041
Neighborhood characteristics				
D_Bus	-0.052	0.027	-0.029	0.046
D_Hospital	0.007	0.033	-0.008	0.067
D_School	-0.064*	0.032	0.075	0.070
D_Government	0.084**	0.029	0.083	0.044
D_Park	-0.105***	0.028	-0.116*	0.048
N_Government	-0.014	0.040	0.076	0.051
N_Park	0.076*	0.033	0.237***	0.045
Street element characteristics				
MVI	0.251***	0.025	0.124***	0.038
BVI	0.051	0.031	-0.219**	0.072
FVI	0.130***	0.035	-0.004	0.044
SVI	-0.258***	0.045	-0.188*	0.078
WVI	-0.021	0.025	-0.041	0.038
GVI	0.272***	0.032	-0.067	0.077

*p < 0.05; **p < 0.01; ***p < 0.001.

Table 3. Regression Coefficients and Standard Errors.

3.3.1 Spatial Scale Analysis: In the MGWR model, variable bandwidths were employed to mitigate scale disparities among variables, reflecting their distinct spatial distributions. Uniform impacts across locations were observed for variables such as GR, D_School, D_Government, D_Park, and N_Park, attributed to globalized bandwidths. Conversely, spatial variability was exhibited by AGE, HS, and D_Hospital, leading to differential impacts on housing prices. Spatial non-uniformity was also demonstrated by visual landscape elements, represented by MVI, BVI, and GVI, resulting in variable effects on housing prices across regions. It was highlighted through statistical analysis in the Mountain View area that variables like N_Park, FVI, SVI, and GVI were impacted globally, indicating consistent effects over larger spatial extents. In contrast, significant spatial heterogeneity was shown by AGE, FR, HS, D_School, and BVI, as evidenced in Table 2.

3.3.2 Regression Coefficient Analysis: In the global regression model presented in Table 3, the analysis underscored how specific factors, including HS and GR, exerted a significant influence on housing prices across various regions. Research by D_Park and N_Park further demonstrated the substantial impact of proximity to parks on price, emphasizing the critical role of environmental considerations in residential choices. Additionally, the MVI emerged as a significant determinant of prices through its influence on street view elements, with its effects exhibiting spatial heterogeneity reflective of distinct neighborhood characteristics. The GVI, while generally positively associated with housing prices, showed a slight negative correlation in mountain view areas in Table 3.

As Table 4 illustrated, in the structural characteristics of both macro scale areas and mountain view areas, the GR emerged as the most significant predictor, indicating appreciable growth in housing prices with increases in GR.

Variables	Model 1 (macro scale)				Model 2 (mountain view)			
	Mean	STD	Min	Max	Mean	STD	Min	Max
Structural characteristics								
<i>AGE</i>	-0.003	0.110	-0.254	0.261	-0.112	0.416	-1.400	0.550
<i>FR</i>	0.044	0.026	-0.019	0.075	0.176	0.140	-0.148	0.528
<i>HS</i>	0.010	0.121	-0.158	0.279	0.043	0.663	-1.697	1.117
<i>GR</i>	0.115	0.004	0.100	0.122	0.257	0.069	0.158	0.333
Neighborhood characteristics								
<i>D_Bus</i>	-0.028	0.073	-0.195	0.059	-0.069	0.133	-0.321	0.281
<i>D_Hospital</i>	0.128	0.231	-0.284	1.078	0.692	0.231	0.370	1.099
<i>D_School</i>	-0.058	0.020	-0.085	-0.010	-0.231	0.457	-1.451	0.793
<i>D_Government</i>	0.076	0.001	0.075	0.080	-0.006	0.102	-0.298	0.171
<i>D_Park</i>	-0.059	0.003	-0.067	-0.056	-0.274	0.319	-0.947	0.346
<i>N_Government</i>	-0.020	0.142	-0.190	0.304	0.146	0.588	-0.541	0.978
<i>N_Park</i>	0.214	0.001	0.212	0.218	0.087	0.002	0.083	0.090
Street element characteristics								
<i>MVI</i>	0.630	0.558	-0.185	1.780	0.045	0.076	-0.018	0.364
<i>BVI</i>	0.153	0.329	-0.560	1.593	-0.041	0.187	-0.448	0.525
<i>FVI</i>	0.054	0.040	-0.001	0.111	0.026	0.016	0.008	0.050
<i>SVI</i>	0.040	0.137	-0.441	0.237	-0.092	0.014	-0.109	-0.072
<i>WVI</i>	-0.019	0.036	-0.057	0.045	0.042	0.041	0.005	0.135
<i>GVI</i>	0.327	0.118	0.325	0.514	-0.037	0.004	-0.047	-0.034

Table 4. MGWR regression coefficient statistical description.

Notably, within neighborhood characteristics, the distance to the nearest park suggested that closer proximity to parks was associated with higher urban housing prices. Furthermore, the number of parks significantly elevated housing prices, with this effect distributed evenly across the area. Parks enriched urban areas with green spaces and provided residents with areas for rest, exercise, and leisure (Helbich et al., 2019), increasing buyers' willingness to invest (Wu et al., 2022). Moreover, accessible transportation could enhance property values in the neighborhood. However, it was noteworthy that for every additional kilometer from bus stops, housing prices could decrease by 2.8% and 6.9%, respectively. Additionally, in areas already afflicted by noise, an excess of bus stops could further aggravate noise pollution and traffic congestion, potentially diminishing property values in those communities.

Our study focused on assessing the impact of mountain urban environment characteristics on housing prices. Incorporating six street view elements' estimated coefficients, we explored their collective influence on housing prices, as depicted in Figure 9. At a macro scale, a unit increase in the MVI corresponded with a substantial 63.0% rise in housing prices, potentially reaching up to 178%. This highlighted the significant influence of mountain view on property values, particularly within the urban core, as shown in Figure 9. The spatial distribution of housing prices among neighborhood clusters revealed MVI's positive impact on central areas, attributed to residents' appreciation for scenic beauty. In contrast, the mountain view area showed a clear preference for the city's northern mountain ridge, extending westward. Despite favorable views, residential preferences shift from the urban core, boosting infrastructure demand in surrounding areas. Significant influences on central housing prices come from indices like the BVI, SVI, and GVI, with the WVI notably higher in the northwest due to abundant lakes and water bodies, thereby raising housing prices. This underscores the combined impact of natural elements like mountains and water on property values. A general trend reveals that the MVI positively correlates with housing price increases, albeit with significant spatial differences. Structural and street

view elements across neighborhoods contribute to property value disparities.

3.3.3 Grad-CAM Visualization Results: The study leveraged Grad-CAM to elucidate focal points in the ConvNeXt model's predictions of satisfaction levels across mountain view images, exploring their implications for housing prices. Figure 10 revealed that in images with higher satisfaction levels, the model primarily highlighted natural features such as mountains and greenery, suggesting that superior mountain views were associated with higher community property values. However, for images with lower satisfaction levels, the model's focus shifted towards flat and architectural elements, indicating that street elements in these instances did not significantly enhance housing prices. Through Grad-CAM visualizations, this analysis provided a fresh perspective on the influence of visual perceptions of natural versus built elements on real estate valuation, highlighting the distinct effects of environmental and architectural factors on housing market dynamics.

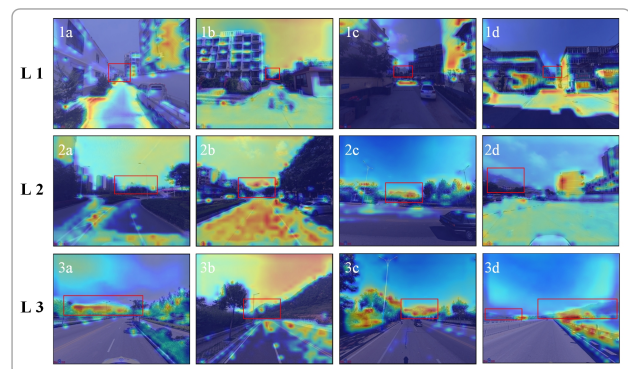


Figure 10. Grad-CAM visualization class activation heat map with mountains marked with boxes.

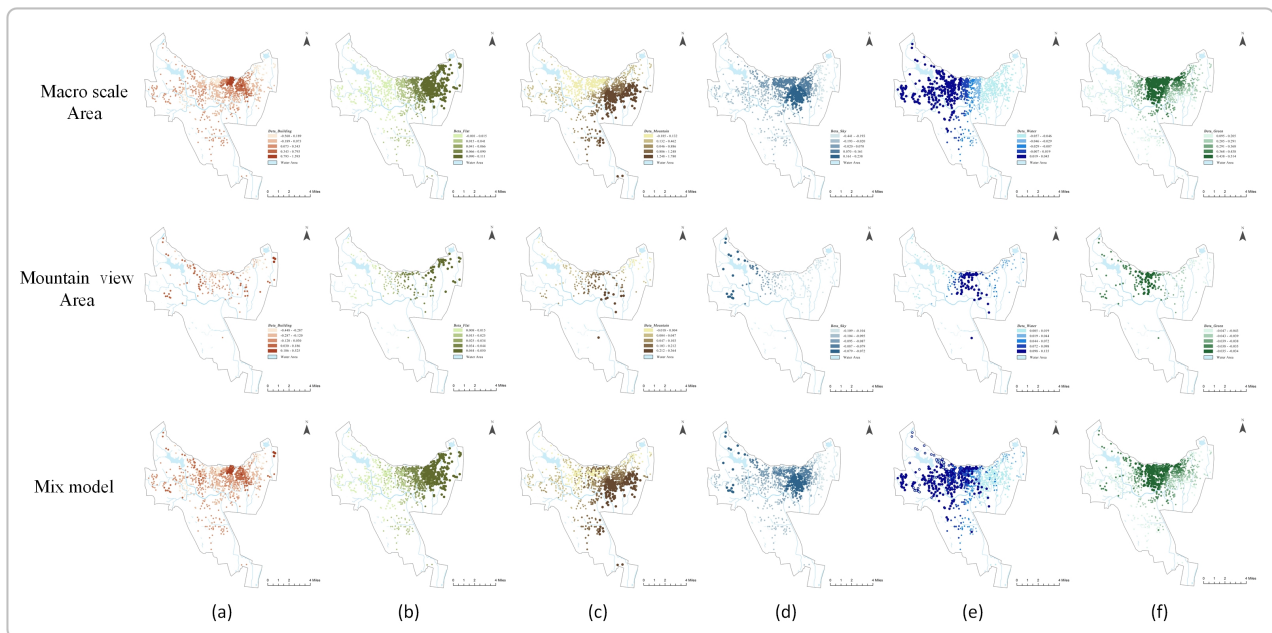


Figure 9. The estimated coefficients for street view element variables. (a) building view index; (b) flat view index; (c) mountain view index; (d) sky view index; (e) water view index; (f) green view index.

4. Conclusion

In this study, we combined SVI, data from varied sources, geographically weighted regression analysis, and deep learning techniques with subjective behavioral perception forecasts to assess how environmental features impact housing prices in mountainous urban areas. Utilizing SVI and open urban data facilitated the analysis of the spatial distribution of urban street view elements. An increase in mountain view and green visibility was found to significantly boost satisfaction ratings for urban streets, despite the uneven distribution of some street view elements. Moreover, the variation in housing prices was scrutinized through the adoption of geographically weighted regression models for both macro scale areas and mountain view areas. This method uncovered varied results, emphasizing the spatial heterogeneity in housing price determinants across different models. Analysis revealed that street view elements significantly impact urban housing prices, with mountain view factors specifically showing pronounced spatial variability in their influence on property values. Finally, based on the subjective evaluations of sample images by volunteers, a human perception model was constructed. Through this, the observational characteristics of Grad-CAM in mountain city street view were explored, aiding in the discussion of a distinct pattern in the distribution of housing prices in cities with mountainous environmental features. It was observed that residents in core residential areas exhibit varying levels of demand for mountain views, with a preference for the accessibility of essential infrastructure, such as transportation and healthcare services. An increase in the mountain view index significantly elevated housing prices, attracting individuals with higher purchasing capacities towards residences with picturesque mountain views. Conversely, in neighboring areas rich in mountain view resources, the influence of additional factors on housing prices was found to be amplified.

This study focuses on housing price evaluation and the factors influencing it in cities with distinct characteristics, aiding in the analysis of property valuation and pricing trends across diverse urban settings. Future work will involve collecting extensive resources and open data, along with in-depth subjective

perception analysis, to enhance our understanding of what affects housing prices in mountain cities.

Acknowledgements

This research was funded by the 2024 Postgraduate Research & Practice Innovation Program of Jiangsu Province (Project Number KYCX24_2978). We would like to thank those who participated in the visual perception questionnaire. In addition, the anonymous reviewers provided valuable comments that significantly improved this paper.

References

- Beza, B.B., 2010. The aesthetic value of a mountain landscape: A study of the Mt. Everest Trek. *Landscape Urban Plan*, 97(4), 306-317.
- Chen, L., Yao, X., Liu, Y., Zhu, Y., Chen, W., Zhao, X., Chi, T., 2020. Measuring Impacts of Urban Environmental Elements on Housing Prices Based on Multisource Data—A Case Study of Shanghai, China. *Isprs Int J Geo-Inf*, 9(2), 106.
- Chin, H.C., Foong, K.W., 2006. Influence of School Accessibility on Housing Values. *J Urban Plan Dev*, 132(3), 120-129.
- Diederik P. Kingma, J.B., 2017. Adam: A Method for Stochastic Optimization.
- Everingham, M., Eslami, S.M.A., Van Gool, L., Williams, C.K.I., Winn, J., Zisserman, A., 2015. The Pascal Visual Object Classes Challenge: A Retrospective. *Int J Comput Vision*, 111(1), 98-136.
- Helbich, M., Yao, Y., Liu, Y., Zhang, J., Liu, P., Wang, R., 2019. Using deep learning to examine street view green and blue

- spaces and their associations with geriatric depression in Beijing, China. *Environ Int*, 126, 107-117.
- Ilya Loshchilov, F.H., 2019. Decoupled Weight Decay Regularization.
- Jim, C.Y.Chen, W.Y., 2006. Impacts of urban environmental elements on residential housing prices in Guangzhou (China). *Landscape Urban Plan*, 78(4), 422-434.
- Jim, C.Y.Chen, W.Y., 2009. Value of scenic views: Hedonic assessment of private housing in Hong Kong. *Landscape Urban Plan*, 91(4), 226-234.
- Joshi, A., Kale, S., Chandel, S.Pal, D., 2015. Likert Scale: Explored and Explained. *British Journal of Applied Science and Technology*, 7(4), 396 - 403.
- Kopczewska, K.Lewandowska, A., 2018. The price for subway access: spatial econometric modelling of office rental rates in London. *Urban Geogr*, 39(10), 1528-1554.
- Liao, X., Deng, M.Huang, H., 2022. Analyzing Multiscale Spatial Relationships between the House Price and Visual Environment Factors. *Applied Sciences*, 12(1), 213.
- Liu, G., Wang, X., Gu, J., Liu, Y.Zhou, T., 2019. Temporal and spatial effects of a 'Shan Shui' landscape on housing price: A case study of Chongqing, China. *Habitat Int*, 94, 102068.
- Liu, P., Zeng, C.Liu, R., 2023. Environmental adaptation of traditional Chinese settlement patterns and its landscape gene mapping. *Habitat Int*, 135, 102808.
- Liu, Z., Mao, H., Wu, C., Feichtenhofer, C., Darrell, T.Xie, S., 2022. A ConvNet for the 2020s.
- Mak, M.Y.Thomas Ng, S., 2005. The art and science of Feng Shui—a study on architects' perception. *Build Environ*, 40(3), 427-434.
- Marquardt, D.W., 1970. Generalized Inverses, Ridge Regression, Biased Linear Estimation, and Nonlinear Estimation. *Technometrics*, 12(3), 591 - 612.
- Neuhold, G., Ollmann, T., Bulo, S.R.Kontschieder, P., 2017. The Mapillary Vistas Dataset for Semantic Understanding of Street Scenes. *IEEE*, pp. 5000-5009.
- Qi, A.N., Huabin, X., Yanxin, G.Junying, W.U., 2022. Landscape Visual Aesthetics Measurement, Assessment, and Improvement of Street Pedestrian Spaces in Mountainous Cities — Case Study on the Historic Downtown of Jinan, Shandong Province. *Landsc Archit Front*, 10(1), 9.
- Sung, H., Lee, S.Jung, S., 2014. Identifying the Relationship between the Objectively Measured Built Environment and Walking Activity in the High-Density and Transit-Oriented City, Seoul, Korea. *Environment and Planning. B, Planning & Design*, 41(4), 637-660.
- Wen, H., Zhang, Y.Zhang, L., 2015. Assessing amenity effects of urban landscapes on housing price in Hangzhou, China. *Urban for Urban Gree*, 14(4), 1017-1026.
- Wu, C., Du, Y., Li, S., Liu, P.Ye, X., 2022. Does visual contact with green space impact housing prices? An integrated approach of machine learning and hedonic modeling based on the perception of green space. *Land Use Policy*, 115, 106048.
- Xie, E., Wang, W., Yu, Z., Anandkumar, A., Alvarez, J.M.Luo, P., 2021. SegFormer: Simple and Efficient Design for Semantic Segmentation with Transformers. *Cornell University Library, arXiv.org, Ithaca*.
- Xu, X., Qiu, W., Li, W., Liu, X., Zhang, Z., Li, X.Luo, D., 2022. Associations between Street-View Perceptions and Housing Prices: Subjective vs. Objective Measures Using Computer Vision and Machine Learning Techniques. *Remote Sens-Basel*, 14(4), 891.
- Yamagata, Y., Murakami, D., Yoshida, T., Seya, H.Kuroda, S., 2016. Value of urban views in a bay city: Hedonic analysis with the spatial multilevel additive regression (SMAR) model. *Landscape Urban Plan*, 151, 89-102.
- Yu, Y., Liu, B., Ma, L., Han, X.Jung, T., 2023. 'Thousand Years of Charm': Exploring the Aesthetic Characteristics of the Mount Tai Landscape from the Cross-Textual Perspective. *Land-Basel*, 12(12), 2129.
- Zhang, J., Zhang, Y., 2019. The evolution and identification of cultural landscape value in protected areas: A case of Mount Tai. *J. Nat. Resour.*, 34(09), 1833-1849.
- Zhao, X., Lu, Y.Lin, G., 2024. An integrated deep learning approach for assessing the visual qualities of built environments utilizing street view images. *Eng Appl Artif Intel*, 130, 107805.

Appendix A

Variables	Description
<i>PRICE</i>	RMB/m ² , dependent variable
Structural characteristics	
<i>AGE</i>	Age of the building
<i>FR</i>	Floor-area ratio
<i>HS</i>	Number of households
<i>GR</i>	Green coverage rate (%)
Neighborhood characteristics	
<i>D_Bus</i>	Distance to the nearest bus stop (km)
<i>D_Hospital</i>	Distance to the nearest hospital (km)
<i>D_School</i>	Distance to the nearest school (km)
<i>D_Government</i>	Distance to the nearest government (km)
<i>D_Park</i>	Distance to the nearest park (km)
<i>N_Government</i>	Number of governments within 1000 m walking distance
<i>N_Park</i>	Number of parks within 1000 m walking distance
Street element characteristics	
<i>MVI</i>	Mountain view index
<i>BVI</i>	Building view index
<i>FVI</i>	Flat view index
<i>SVI</i>	Sky view index
<i>WVI</i>	Water view index
<i>GVI</i>	Green view index

Table A1. Descriptive statistics of variables.